02

Anisotropic saturation of the EPR spectrum of an DCO radical stabilized in solid CO at 4.2 K and its orientation motion

© Ya. A. Dmitriev

Ioffe Institute,
St. Petersburg, Russia

e-mail: dmitriev.mares@mail.ioffe.ru

Received May 25, 2022
Revised October 7, 2022
Accepted October 14, 2022

Formyl radicals, DCO, were produced in solid CO matrix and studied by EPR using gas deposition technique on a cold substrate at 4.2 K. The radical electron spin-lattice relaxation was measured to be anisotropic. The anisotropy was found to originate from the anisotropic orientational motion of the radical with the most intensive librations performed around a z axis corresponding to the smallest moment of inertia of the molecule. It was shown that, in solid CO, the libration motion of small molecules is modeled by considering a particle rotating in the orientational potential box. A suggestion was substantiated about the complicated nature of the orientational motion of HCO in the solid CO matrix including the intensive librations and slow tunneling rotation of the molecule around the z axis.

Keywords: electron paramagnetic resonance, matrix isolation, formyl radical, anisotropy of the spin-lattice relaxation time, librations and tunneling rotation of molecules.

DOI: 10.21883/EOS.2022.12.55238.3712-22

Introduction

The work is devoted to the experimental study of formyl radicals on the example of a DCO radical matrix isolated at cryogenic temperatures. The need to know the properties of the formyl radical is determined by the fact that it is an important intermediate particle in a wide range of chemical reactions. In such, for example, as the formation of complex organic molecules in the icy mantles of cosmic dust [1], in the combustion of hydrocarbon flame [2], in atmospheric chemical reactions involving organic molecules [3]. The particle under study is paramagnetic, which determines the use of the electron paramagnetic resonance (EPR) method, which is the most sensitive and informative in this case. The combination of EPR detection with the technique of low-temperature matrix isolation makes it possible to obtain and study chemically highly active radicals in sufficiently large spin concentrations to achieve a high signal-to-noise ratio, which is critical for a thorough study of the radical structure, its dynamics, and features of interaction with the matrix environment. Moreover, matrix isolation is used to simulate low-temperature chemical processes occurring on grains in interstellar dust clouds [4,5].

In the recent work [6], high-resolution EPR spectra of HCO and DCO radicals in solid CO were obtained at temperatures of 1.4–4.2 K. The spectra were modeled and the experimental values of the components of the g- and A-tensors, as well as individual line widths, were determined. With the involvement of a dozen and a half theoretical methods, both *ab initio* and DFT, the structure of molecules, their vibrational spectra and the parameters of the EPR spectra were calculated, taking into account the influence of vibrational modes on these parameters. A significant contribution of vibrational modes, and especially those that change the position of the proton (deuteron), to the isotropic component of the hyperfine structure tensor (A-tensor) has been found, which leads to its significant increase compared to the design base value for a rigid molecule and the deviation of the ratios of these isotropic components for HCO and DCO from the ratio of g-proton and deuteron factors, $g_n(H)/g_n(D) = 6.514$. This isotopic effect in the isotropic component of the A tensor is reliably recorded in the experiment: $(A^H_{iso}/A^D_{iso})_{\exp} = 6.77$. By comparing experimental and theoretical results, estimates of the amplitudes of valence and deformation vibrations for a light formyl radical HCO are obtained. As for the matrix shift of parameters, it is also significant in relation to A_{iso}, but it is not noticeable in the anisotropic components of the HFC tensor and in the components of the g tensor. At the same time, the anisotropy of the g-tensor is partially averaged by librations or tunneling rotational motion of the formyl radical around the axis of the inertia tensor with the smallest eigenvalue. Estimates of libration amplitudes are obtained within the libration model [6]: 21.14° for HCO and 14.08° for DCO. Within the framework of the rotational model, the correlation time of the rotational motion $\tau_c = 20$ ns is determined by modeling the spectra.

It should be noted that the dynamics of the radical is clearly reflected in the parameters of the EPR spectrum of a light molecule, HCO, and is insufficiently expressed in the parameters of the DCO spectrum, which is associated with both a smaller amplitude of the intramolecular motion of the D atom compared to the H atom and a lower intensity of

the orientation motion of the DCO compared to the HCO, and with a lower resolution of the hyperfine structure of the DCO spectrum due to the smaller magnetic moment of the deuteron. The objective of this experimental work was to detect the intense tunnel orientation movement of the stabilized radical DCO and to clarify its librational or rotational nature.

Experimental procedure

The experimental setup and the experimental technique were described in detail earlier in [7]. Below is a short description of them. The samples were obtained by condensation on a cold substrate of two gas streams: one of which was a molecular D_2 passed through an electrodeless discharge at a frequency of 15 MHz, and the other — matrix CO supplied to the substrate bypassing the gas discharge. Both the discharge and the matrix gas were cooled to the temperature of liquid nitrogen. The sample was formed on the surface of a quartz finger located in the center of a cylindrical resonator tuned to the mode TE_{011}. The finger was cooled with liquid helium, the temperature of which was regulated in the range of 1.2−4.2 K by pumping vapor from a tank with liquid He. High purity gaseous CO was used, in which the hard-to-separate N_2 gave a contribution of 1%. Molecular deuterium was purified by passing the source gas through the heated wall of the Pd-Ag alloy tube. Formyl radicals were formed in the matrix in a tunnel reaction of addition of atomic deuterium to CO molecules: $D + CO \rightarrow DCO$. In the experiment, an extremely small flow of deuterium gas was used in order to avoid further hydrogenation of carbon monoxide [7,8] and to stop this chain of reactions at the first stage — formation of a formyl radical [9,10]. This is especially important for observing the EPR of the DCO radical triplet located in the magnetic field in the region of $g \approx 2.0$ and the distance between the hyperfine components of which is less than for the HCO doublet. Based on the gas flow rate the storage balloons with D_2 and CO, as well as on the geometry of the gas deposition system near the substrate, we estimated the gas flows to the substrate: 0.1 mmol/h from the discharge tube (deuterium) and 3 mmol/h via the matrix channel (CO). Microwave power from the klystron is supplied to the resonator through an attenuator, which allows you to adjust the amplitude of the resonant magnetic field in the resonator in a wide range. The power incident on the attenuator is 15 mW.

Experimental results and discussion

Fig. 1 shows the EPR spectrum of the DCO radical stabilized in the CO matrix at 4.2 K. In the experiment, the amplitudes of the spectra corresponding to those shown in Fig. 1, *a* and Fig. 1, *c* are very different. In Fig. 1, they are aligned in order to make the change in the shape of the lines more visible. A characteristic feature of the spectrum

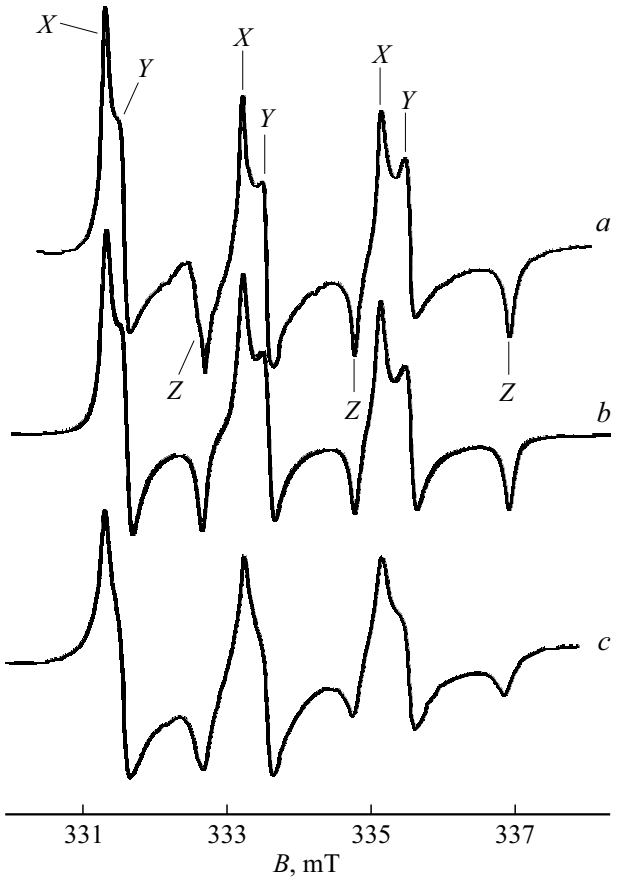

Figure 1. The EPR spectrum of the DCO radical stabilized in the CO matrix at 4.2 K. The resonance frequency of the spectrometer, $f_{res} = 9347.53$ MHz. *a* — experimental spectrum recorded with the attenuation of the power of the electromagnetic wave entering the microwave resonator equal to 50 dB; *b* — simulated using the program EasySpin unsaturated spectrum of DCO (spin-Hamiltonian parameters are specified in the text); *c* — experimental spectrum recorded with attenuation of microwave power equal to 30 dB.

is the presence of three components with a distance in the magnetic field between neighboring components of about 20 G. This structure of the spectrum reflects the interaction of an unpaired radical electron with the nucleus of a deuterium atom with spin $I = 1$. It can be seen from the figure that both the hyperfine interaction tensor, *A*, and the *g* tensor have pronounced anisotropy with different eigenvalues along the three main axes. The simulation was performed with the use of the spin-Hamiltonian parameters in the inertia Cartesian principal frame [6] which were empirically obtained and listed in Table 1. The axis *z* of this coordinate system lies in the plane of the molecule and is directed at a slight angle to the valence bond C = O, the axis *y* — in the same plane, the axis *x* is perpendicular to the plane of the molecule.

With an increase in the microwave power of the resonant magnetic field, the EPR lines of the radical broaden, and their amplitude changes non-linearly depending on the

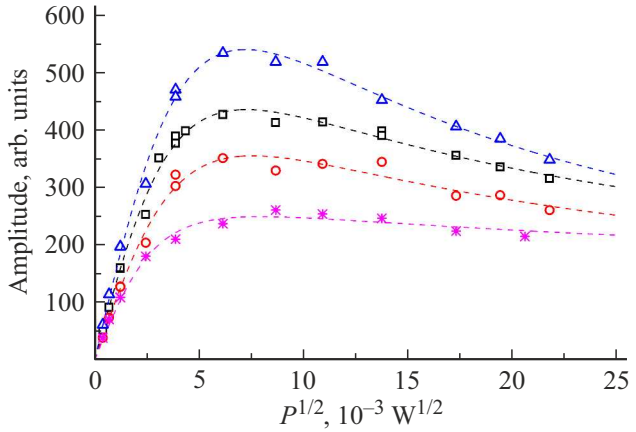

Figure 2. The symbols indicate experimental data on the microwave saturation of the resonance lines of the EPR spectrum of the DCO radical, Fig. 1. Here are blue triangles, black squares and red circles — data for resonances corresponding to the X- and Y-components of the g-tensor (g_{xx} and g_{yy}), which are determined from recordings of the low-field, middle and high-field hyperfine transitions, respectively purple snowflakes — data for the resonance of a upfield line corresponding to the Z component of the g tensor. The dashed fitting lines are calculated using the three-parameter formula described in the text.

Table 1. Components of g- and A-tensors used in simulating the EPR spectrum of the DCO radical, Fig. 1, *b*. The individual line has a Lorentz shape and a width (between the extremes of the first derivative) of 0.095 mT. Resonance frequency, $f_{res} = 9347.53$ MHz

Tensor		Components		
		X	Y	Z
g	X	2.004268	0.0000028	−0.0000026
	Y	0.0000028	2.0020339	0.0005632
	Z	−0.0000026	0.0005632	1.9949954
A, G	X	19.031	−0.0013	0.0011
	Y	−0.0013	19.8153	−0.8135
	Z	0.0012	−0.8135	21.0877

square root of the power. Fig. 2 shows the dependences of the amplitudes of various components of the hyperfine transitions on $P^{1/2}$, where P — the power of the microwave wave supplied to the resonator.

To fit the experimental data on line saturation, the three-parameter ratio [11,12] was used:

$$A = \frac{P_1 P^{1/2}}{(1 + P/P_2)^{P_3}}. \quad (1)$$

Here P — the power of the resonant microwave magnetic field, P_1, P_2, P_3 — fitting parameters. The value P_1 is proportional to the gain of the amplifying path of the spectrometer, P_3 — parameter taking into account the shape of the spectrum line: $P_3 = 3/2$ line for the first-derivative of a homogeneous absorption line, $P_3 = 1$ for the absorption line (zero-order derivative), $P_3 = 1/2$ for a completely inhomogeneous absorption derivative. P_2 — the saturation parameter is inversely proportional to the spin-lattice relaxation time, T_1, and the spin-spin relaxation time, T_2. The value of the microwave field power corresponding to the maximum of the absorption curve is calculated as

$$P_{\max} = \frac{P_2}{2P_3 - 1}. \quad (2)$$

The fitting curves shown in Fig. 2 are calculated for the values of the parameters P_1, P_2, P_3 listed in Table 2. These parameter values are obtained from experimental data using the least squares method.

An estimate of the spin-lattice relaxation time T_1 can be obtained using the relation [13]:

$$T_1 = \frac{1.97 \cdot 10^{-7} \Delta H_{ms}}{g H_1^2}.$$

Here ΔH_{ms} — the width of the line (in Gauss) measured between the extremes of the first derivative, H_1 — the amplitude of the magnetic component (in Gauss) of the resonant microwave field corresponding to the maximum of the absorption curve, T_1 — time (in seconds) of spin-lattice relaxation. As a result, the values of T_1 determined by the XY resonances of the low-field, middle and high-field lines are equal to, respectively, $8.935 \cdot 10^{-6}$, $8.828 \cdot 10^{-6}$, $8.096 \cdot 10^{-6}$ s. After averaging over three hyperfine components, we have, $T_1^{XY} = 8.62(37) \cdot 10^{-6}$ s, in comparison with the value $T_1^Z = 7.31 \cdot 10^{-6}$ s, determined from the records of the Z resonance of the high-field line.

Thus, anisotropy of the electron spin-lattice relaxation time for the DCO radical stabilized in the CO matrix is observed in the experiment. It is known that the limitations of the spatial motion of the spin probe can lead to anisotropy of the spin-spin and spin-lattice relaxation times. In most of the works, this phenomenon was observed when recording NMR spectra. So, the authors of the works [14,15] found anisotropy T_1 in NMR spectra of hydrogen nuclei in liquids in nanopores smaller than 700 nm, and having axial symmetry. The relaxation times determined by the interaction of the probe and the walls of nanopores experiencing fluctuation movements differed by orders of magnitude in the cases of a magnetic field oriented along the axis of symmetry of the cell and perpendicular to this axis. In the condensed state, hexamethylbenzene molecules perform intensive orientational movement around six-fold axis („C_6-movement“) over a wide temperature range. As a result of this anisotropic reorientation, the time of the nuclear spin-lattice relaxation shows a strong dependence on the six-fold axes orientation to the applied magnetic field [16]. In the work cited above, deuterated samples were studied. As a result of the „C_6-motion“ fluctuations of the quadrupole interaction of deuterium nuclei responsible for spin-lattice relaxation occurred. In the work [17], the anisotropy of the relaxation times T_1 and T_2 of the nuclear magnetic resonance of water protons in skeletal

Table 2. Parameters P_1, P_2, P_3, determined from experimental data and used to calculate saturation curves, Fig. 2, in accordance with the formula (1). The table also shows the values of $P_{\max}$, formula (2), corresponding to the abscissas of the maxima of the theoretical saturation curves in Fig. 2 and calculated using the formula (2)

Resonances, corresponding to components of the g-tensor	Superfine line	Parameters			
		P_1	P_2	P_3	$P_{\max}$
XY	Low-field	155.92808	40.90017	0.89364	51.95124
	Middle	134.69104	28.31195	0.76924	52.57753
	High-field	105.4297	30.50075	0.766	57.33224
Z	Upfield	93.0594	10.64649	0.56595	63.513

muscles was studied. The nature of anisotropy is the partial orientation of water molecules when they interact with actomyosin filaments. When studying nitroxide radicals, it was found [18] that the electron spin-lattice relaxation time, measured at various points of the EPR line at 6 K, varies by more than an order of magnitude. It is noted that for nitroxide radicals, the coupling of electrons with the phonons of the matrix is carried out mainly through the spin-orbit interaction of unpaired electrons [18]. The possible mechanisms of electron spin relaxation associated with the movement of molecules have by their nature the modulation of the following parameters and interactions: hyperfine interaction anisotropy, g-tensor anisotropy, spin-rotational interaction, dipole-dipole interaction [19].

It is reasonably assumed that the T1 anisotropy in our case originates in the intensive reorientation of the DCO molecule preferably around the principal z' axis of the inertia tensor [6], relating to the DCO smallest momentum of inertia. The small moment of inertia contributes to the manifestation of quantum tunneling in orientation motion at helium sample temperatures. We estimate the contribution of the anisotropic reorientation of the DCO molecule to the anisotropy of the relaxation time T_1 in order of magnitude. The contributions of the isotropic and anisotropic components can be analyzed by representing the relaxation rate as the sum of the corresponding components [17]:

$$\frac{1}{T_1} = \frac{1}{T_{1,iso}} + \frac{1}{T_{1,aniso}}. \tag{3}$$

In our case $T_1 = T_1^Z$, $T_{1,iso} = T_1^{XY}$. As a result, we find $T_{1,aniso} = 4.8 \cdot 10^{-5}$ s.

To determine the mechanisms that can make a significant contribution to $T_{1,aniso}$, we will use as ordinal estimates of the effect of the isotropic Brownian rotational motion [20,21] on the relaxation time. At cryogenic temperatures, there is no population of excited rotational levels of the molecule and, consequently, the contribution of the Hamiltonian corresponding to the spin-rotational mechanism, $H^{SR} = \hbar \mathbf{S} \cdot \mathbf{C} \cdot \mathbf{J}$, is equal to zero. In the given expression $\mathbf{S}$ and $\mathbf{J}$ — vectors corresponding to the electron spin and angular momentum of the molecule.

Contribution of the g-tensor anisotropy modulation:

$$(T^g_{1,aniso})^{-1} = \frac{2}{5}\left(\frac{\mu_B \omega}{g\beta}\right)^2 \left[\frac{(\Delta g)^2}{3} + (\delta g)^2\right] \frac{\tau_c}{1 + (\omega\tau_c)^2}, \tag{4}$$

where $\Delta g = g_{zz} - 0.5(g_{xx} + g_{yy})$, $\delta g = 0.5(g_{xx} - g_{yy})$; μ_B — Bohr electron magneton; i — enumeration of Cartesian projections x, y, z; $g_e = 2.0023$, and the relaxation rate does not depend on the resonance frequency.

For the contribution of the modulation of the anisotropy of the hyperfine interaction (A-tensor) we have

$$(T^A_{1,aniso})^{-1} = \frac{1}{6}\sum_{i=1}^{3}(A_i - \bar{A})^2 \frac{\tau_c}{1 + (\omega\tau_c)^2}. \tag{5}$$

Here i — enumeration of Cartesian projections x, y, z; $\omega = 2\pi f_{res}$ — resonance circular frequency.

The greatest contribution to the relaxation rate is achieved at $\omega\tau_c = 1$, i.e. at modulation frequencies near the Larmor frequency and, accordingly, the correlation time $\tau_c = 1.7 \cdot 10^{-11}$ s. It is obvious that the tunneling rotational reorientation with correlation time [6]$\tau_c = 20$ ns does not make a noticeable contribution to spin-lattice relaxation. Based on the obtained experimental estimate of $T_{1,aniso}$, formula (3), and the contribution to the relaxation rate of the modulation of the anisotropy of the g tensor, formula (4), we obtain for the correlation time $\tau_c^g = 2.64 \cdot 10^{-12}$ s and, accordingly, the modulation frequency value is $3.8 \cdot 10^{11}$ Hz. In this case, the formula (5) demonstrates a negligible contribution of the A-tensor anisotropy modulation to the relaxation rate: $T^A_{1,aniso} = 0.137$ s. Based on the obtained correlation time τ_c^g and the estimate of the libration amplitude DCO 14.08° (see Introduction), the libration frequency necessary to achieve the required relaxation rate can be roughly estimated as $3.8 \cdot 10^{11}(360°/4 \cdot 14.08°) = 2.4 \cdot 10^{12}$ Hz. Here, the expression in parentheses is the ratio of the reorientation angles passed in one rotation and one libration periods.

In the work [22] it was shown that in solid inert gases and *para*-H_2, the anisotropy of the EPR spectrum of the radical CH_3 is determined by the Pauli repulsion forces between the impurity radical and matrix particles. It is

reasonable to assume that the same conclusion holds in the case of matrices of linear molecules. The valence forces are short-ranged. Therefore, we will consider the DCO molecule as performing an oscillatory motion in a potential field as follows: $U(\theta) = 0$ at $|\theta| < \theta_0$ and $U(\theta) = \infty$ when $|\theta| > \theta_0$. Let us estimate the libration frequency of the DCO molecule in the model of a potential orientation box. The value of the square of the sine of the oscillation angle averaged over the energy levels of the particle in this potential box is given by the following expression [23]:

$$\langle \sin^2(\theta) \rangle = \left(\frac{1}{2} - \frac{\sin(2\theta_0)}{4\theta_0} \right) + \frac{\sin(2\theta_0)}{4\theta_0} \sum_{n=1}^{\infty} \frac{W_n}{1 - (\frac{\pi n}{2\theta_0})^2},$$

where $n = 1, 2, 3, \ldots$, and the probability of finding a system in a state with a quantum number of n at a temperature T has the form

$$W_n = \exp\left[-(n^2 - 1)\beta\right] - \exp\left\{-[(n+1)^2 - 1]\beta\right\}$$

at

$$\beta = \frac{h^2}{32 I \theta_0^2 k T}.$$

The component I_z of the inertia tensor of the radical DCO for rotation around the axis z is $I_z = 1.2 \cdot 10^{-47}$ kg·m^2. Libration energy levels are given by the formula [23]:

$$E_n = \frac{n^2}{32} \frac{h^2}{I \theta_0^2}.$$

For the amplitude of librations 14.08°, we get the following estimate of the width of the potential box: $\theta_0 = 39.5°$. For the energy of the ground state of libration motion and the oscillation frequency, we have, respectively, 173.4 K and $3.2 \cdot 10^{12}$ Hz. The obtained frequency value correlates well with the frequency estimate given above when considering the spin-lattice relaxation time: $2.4 \cdot 10^{12}$ Hz.

Earlier [24] the orientation potential box model was used to describe librations around the two-fold axes, C_2, of the methyl radical CH_3 trapped in matrices of linear molecules, N_2, CO, N_2O, CO_2. The libration amplitudes were estimated based on the analysis of partial averaging of the anisotropy of the STS tensor by the reorientation of the molecule. The obtained values of amplitudes, 19.63°, 16.92°, 9.06°, 5.20°, for CH_3, in the matrices N_2, CO, N_2O, CO_2, respectively, turned out to be surprisingly close to the averaged angular deviations of matrix molecules [25]: 19.49°, 14.67°, 5.57°, 5.17°. At low temperatures with only the ground libration level populated, the amplitude of the librations of the molecule in the potential box does not depend on the inertia tensor of the molecule and is determined only by the width of the box [23], which in turn is different for different matrices. The inertia moments of CO, CH_3, DCO are equal to $14.76 \cdot 10^{-47}$, $2.97 \cdot 10^{-47}$, $1.20 \cdot 10^{-47}$ kg·m^2 respectively. The inertia moments differ significantly while the low-temperature libration amplitudes are nearly the same: 14.67°, 16.92°, 14.08°. This circumstance testifies in favor of the applicability of the potential box model. At the same time, the libration amplitude of HCO in CO, equal to 21.14°, is noticeably greater than those listed, despite the fact that the moment of inertia of the light formyl radical, $0.74 \cdot 10^{-47}$ kg·m^2, fits perfectly in a number of the moments of inertia given above. For the convenience of evaluation, the listed information is collected in Table 3.

Table 3. Moments of inertia of molecules, I, and amplitudes of low-temperature librations of these molecules, θ, in solid CO

Molecule	I, 10^{-47} kg·m^2	θ, grad	Ref.
CO	14.76	14.67	[28]
CH_3	2.97	16.92	[27]
DCO	1.20	14.08	[6]
HCO	0.74	21.14	[6]

The noted discrepancy can be explained as follows. In the work [26] it was found that the orientation motion of the radical CH_3 around the axes C_2 has a complex nature: in addition to fast librations, an ultra-slow anisotropic tunneling rotation is observed with a correlation time estimated at several hundred nanoseconds. Such a low rotation speed does not affect the averaging of the anisotropy of the HFC tensor, however, it manifests itself in the averaging of the anisotropy of the line width tensor. In the case of stabilized formyl radicals under consideration, the expected amplitude of librations 14−15° for HCO in an orientation potential box in solid CO is not sufficient for the observed averaging of the anisotropy of the g tensor. It should be assumed that, as in the case of CH_3 in CO, the HCO molecule in solid carbon monoxide performs a complex reorientation around the z axis, which represents rapid librations and tunneling rotation with a correlation time of several tens of nanoseconds, making an additional contribution in relation to librations to averaging the anisotropy of the g tensor. In the case of the heavy formyl radical DCO in the CO matrix, this additional rotation is much slower and does not manifest itself in the spectrum.

Conclusions

Very recently [6], the comparative analysis of the EPR spectra of HCO and DCO trapped in solid CO at helium temperatures supported by theoretical computation of the spectrum parameters was presented. It led to the discovery of the prominent contribution of both the intramolecular vibrational motion of formyl radical and the zero-point orientational motion of the molecule as a solid rotator to the measured parameters. These effects were clearly observed in the spectrum of the light isotope HCO, but were not pronounced in the spectrum of DCO due to the much smaller hyperfine splitting of the lines and the accuracy of theoretical calculations not sufficient in this case. In the

present work, an anisotropy of the time of the electron spin-lattice relaxation of the DCO radical in solid CO at 4.2 K is found, which is based on the well-expressed anisotropic nature of the libration motion of the deuterated molecule. The discovered effect is a manifestation of the dynamics of zero motions in the EPR spectrum of a stabilized radical and is also of interest for the theory of magnetic resonance spectroscopy, since the anisotropy of T_1 has rarely been observed at helium temperatures.

The theory of orientation motion of both matrix and impurity molecules in solids obviously needs further development. The most interesting is the case of van der Waals solids at cryogenic temperatures, when correlation of angular motion and, in particular, quantum tunneling of matrix molecules and impurity particle [27,28] is possible. It should be assumed that when an impurity particle is embedded in the substitutional position of the van der Waals crystal lattice, „adaptation " (relaxation) of the matrix and the impurity particle itself occurs, which for an impurity particle can manifest itself, for example, in a change in its symmetry [27–29].

Acknowledgments

The author is grateful to his colleague and co-author of many papers, Dr. N.P. Benetis, for the information about the inertia tensors of HCO and DCO molecules obtained by calculation by the B3LYP-Pople method.

Conflict of interest

The author declares that he has no conflict of interest.

References

[1] T. Butscher, F. Duvernay, G. Danger, R. Torro, G. Lucas, Y. Carissan, D. Hagebaum-Reignier, T. Chiavassa. Mon. Not. R. Astron. Soc., **486** (2), 1953 (2019).
[2] N.J. Labbe, R. Sivaramakrishnan, C.F. Goldsmith, Y. Georgievskii, J.A. Miller, S.J. Klippenstein. J. Phys. Chem. Lett., **7** (1), 85 (2016).
[3] R. Atkinson. Atmos. Environ., **24** (1), 1 (1990).
[4] N. Watanabe, A. Kouchi. Prog. Surf. Sci., **83** (10−12), 439 (2008).
[5] A.G.G.M. Tielens. Rev. Mod. Phys., **85** (3), 1021 (2013).
[6] Yu.A. Dmitriev, A. Laaksonen, N.P. Benetis. AIP Advances, **10**, 125309 (2020).
[7] R.A. Zhitnikov, Y.A. Dmitriev. Astron. Astrophys., **386** (3), 1129 (2002).
[8] D.E. Woon. Astrophys. J., **569** (1), 541 (2002).
[9] G.W. Fuchs, H.M. Cuppen, S. Ioppolo, C. Romanzin, S.E. Bisschop, S. Andersson, E.F. van Dishoeck, H. Linnartz. Astron. Astrophys., **505** (2), 629 (2009).
[10] N. Watanabe, A. Kouchi. Astrophys. J., **571** (2), L173 (2002).
[11] D.A. Haas, C. Mailer, B.H. Robinson. Biophys. J., **64** (3), 594 (1993).
[12] R.D. Nielsen, S. Canaan, J.A. Gladden, M.H. Gelb, C. Mailer, B.H. Robinson. J. Magn. Res., **169** (1), 129 (2004).
[13] H. Pool. *Tekhnika EPR-Spektroskopii (The EPR spectroscopy technique)* (Mir, M., 1970).
[14] G. Furman, V. Meerovich, V. Sokolovsky, Y. Xia. J. Magn. Res., **311**, 106669 (2020).
[15] G. Furman, S. Goren, V. Meerovich, A. Panich, V. Sokolovsky, Y. Xia. J. Magn. Res., **331**, 107051 (2021).
[16] J. Tang, L. Sterna, A. Pines. J. Magn. Res., **41**, 389 (1980).
[17] S.R. Kasturi, D.C. Chang, C.F. Hazlewood. Biophys. J., **30** (3), 369 (1980).
[18] E.M.M. Weber, H. Vezin, J.G. Kempf, G. Bodenhausen, D. Abergeł, D. Kurzbach. Phys. Chem. Chem. Phys., **19** (24), 16087 (2017).
[19] T.N. Makarov, E.G. Bagryanskaya, H. Paul. Appl. Magn. Res., **26** (1−2), 197 (2004).
[20] B.H. Robinson, D.A. Haas, C. Mailer. Science, **263**, 490 (1994).
[21] J.R. Biller, H. Elajaili, V. Meyer, G.M. Rosen, S.S. Eaton, G.R. Eaton. J. Magn. Reson., **236**, 47 (2013).
[22] Yu.A. Dmitriev, N.P. Benetis. J. Phys. Chem. A, **114**, 10732 (2010).
[23] I.D. Mikheikin, G.M. Zhidomirov. Teor. eksp. khim., **12** (2), 245 (1976). (in Russian).
[24] Yu.A. Dmitriev, V.D. Melnikov, K.G. Styrov, M.A. Tumanova. Physica B, **440**, 104 (2014).
[25] *Cryocrystals*, ed. B.I. Verkina, A.F. Prikhotko (Naukova Dumka, Kiev, 1983).
[26] Yu.A. Dmitriev, V.D. Melnikov, K.G. Styrov, M.A. Tumanova. Physica B, **449**, 25 (2014).
[27] Yu.A. Dmitriev, N.P. Benetis. J. Phys. Chem. A, **122**, 9483 (2018).
[28] Yu.A. Dmitriev. Opt. i spektr., **129** (9), 1129 (2021).(in Russian).
[29] R.E. Asfin, M.V. Buturlimova, T.D. Kolomiytsova, I.K. Tokhadze, K.G. Tokhadze, D.N. Shchepkin. Opt. i spektr., **128** (10), 1478 (2020). (in Russian).